· U · C · UNIVERSIDADE DE COIMBRA

Modelling concentrated fiber suspension flow using different low Reynolds *k*-ε turbulence models

M.G. Rasteiro*, D. Asendrych, F. Garcia, P. Ferreira, P. Faia, C. Cotas

COST ACTION FP1005
(6th ERCOFTAC SIG43 Workshop)

23-25 October 2013, Udine, Italy

1. Objectives
2. Experimental data
3. Geometry
4. Low-Reynolds *k*-ε model
5. Numerical Results
6. Conclusions
7. Future Work

Development of a mathematical model to describe properly the **flow of fiber suspensions in pipes**

- Modelling of fiber suspensions flow in pipes
- Adapt low-Reynolds *k-ε* turbulence models to take into account the presence of fibers
- Validation of the model

Rheological Data

Apparent viscosity of the pulp fiber suspension

$$\eta_{app} = K\left(\dot{\gamma}\right)^{n-1}$$

η_{app} – apparent viscosity

$\dot{\gamma}$ – shear rate

K – consistency coefficient

n – flow behavior index

Table 1– Rheological data for the *Eucalyptus* pulp suspensions tested.

c (% w/w)	*K*	*n*
1.50	0.2798	0.532
1.80	0.5123	0.518
2.50	10.721	0.247

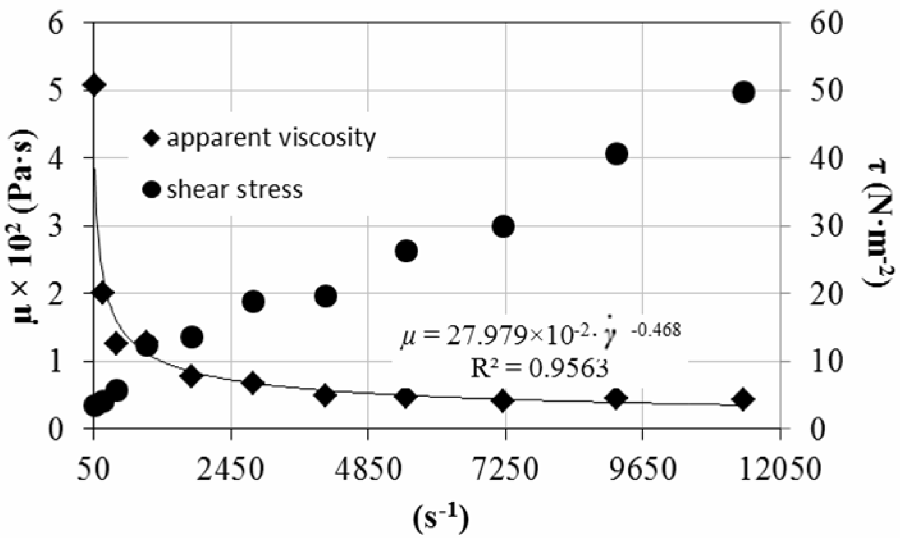

Figure 1 – Rheogram and apparent viscosity for pulp suspension of eucalyptus fibers (c=1.50% w/w).

Experimental Data

Eucalyptus pulp suspension

Fiber length = 0.706 mm
ρ = 998.2 kg·m^{-3}

Crowding factor

$$N = \frac{2}{3} c_v \left(\frac{L_{fiber}}{D_{fiber}} \right)^2$$

- Fiber length, L_{fiber} = 0.706 mm
- Mean fiber diameter, D_{fiber} = 16 μm

Table 2– Experimental information.

c (% w/w)	**1.50**		**1.80**		**2.50**	
U_{in} (m·s^{-1})	4.19	6.21	4.46	6.23	4.90	5.55
$\Delta P/L_{exp.}$ (Pa·m^{-1})	829.1	1288.7	842.6	1203.2	2299.3	2814.3
***N* Crowding Factor**	1947		2336		3245	

Experimental Data

- **Flow rig**: test section (D=7.62cm, L=4m); magnetic flowmeter; differential pressure meter; temperature control and EIT rings.
- **Main results**: pressure drop, fibers distribution and velocity profiles.

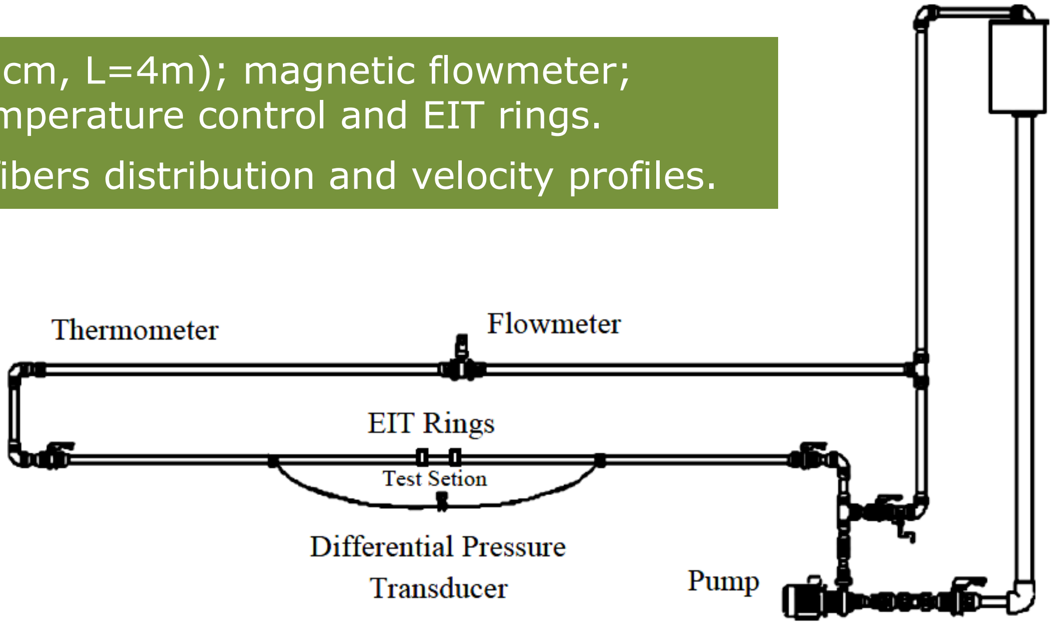

Figure 2 - Schematic view of the pilot rig (adapted from Ventura *et al* (2008) and Faia *et al* (2012)).

Figure 3 - Pilot rig existent (adapted from Rasteiro (2011)).

Faia, P.; Silva, R.; Rasteiro, M.; Garcia, F.; Ferreira, A.; Santos, M.; Santos, J.; Coimbra, P. (2012) – *"Imaging Particulate Two-Phase Flow in Liquid Suspensions with Electric Impedance Tomography"* – Particulate Science and Technology, 30(4): 329-342
Rasteiro, M. (2011) – "*Modelling Fiber suspensions Flows Using Rheological Data*". COST Action FP1005 meeting, Nancy, 13-14 October
Ventura, C.; Garcia, F.; Ferreira, P.; Rasteiro, M. (2008) – *"Flow Dynamics of Pulp Fiber suspensions"* – TAPPI Journal, 7(8): 20-26

3. Geometry

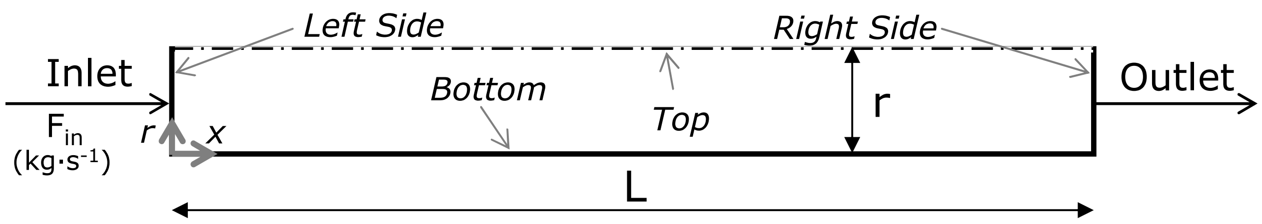

Figure 4 – Geometry and boundaries.

r = 0.0381 m

L = 1 m

Table 3– Boundary conditions.

Location	Boundary Condition
Left Side	Periodic Boundary
Right Side	Periodic Boundary
Top	Axis
Bottom	Wall

The pulp flow is assumed as:

-Steady state (fully developed flow)

- Isothermal

- Without mass transfer;

- Incompressible

- 2D flow with axial symmetry

- Viscosity was considered dependent on shear rate

It was considered a water annulus at the wall with thickness equal to fiber length

Complete set of differential equations

- *Standard k-ε turbulence model*

General transport equation

$$\frac{\partial}{\partial x_i}(\rho u_i \phi) = \frac{\partial}{\partial x_i}\left(\Gamma_\phi \frac{\partial \phi}{\partial x_i}\right) + S_\phi$$

Cartesian Coordinates
Steady state
2D geometry

Table 4– Expressions for the dependent variable, diffusibility term Γ_Φ and source-term S_Φ (Costa et al. 1999).

Transported property	ϕ	Γ_ϕ	S_ϕ
Mass	1	0	0
Momentum in *i*-direction	u_i	$\mu_{ef} = \mu + \mu_t$	$-\frac{\partial p_{ef}}{\partial x_i} - g_i \beta\rho(T - T_{ref}) + \frac{\partial}{\partial x_j}\left(\rho\mu_{ef}\frac{\partial u_j}{\partial x_i}\right)$
Turbulent kinetic energy	k	$\mu_{ef} = \mu + \frac{\mu_t}{\sigma_k}$	$P_k + G_k - \rho\varepsilon + D_k$
Dissipation rate of k	ε	$\mu_{ef} = \mu + \frac{\mu_t}{\sigma_\varepsilon}$	$\rho\frac{\varepsilon}{k}(f_1 C_{\varepsilon 1} P_k - f_2 C_{\varepsilon 2}\varepsilon + C_{\varepsilon 1} C_{\varepsilon 3} G_k) + E_\varepsilon$

$$\mu_t = \rho C_\mu \frac{k^2}{\varepsilon}$$

$$P_k = \rho\mu_t\left(\frac{\partial u_i}{\partial x_j} + \frac{\partial u_j}{\partial x_i}\right)\frac{\partial u_i}{\partial x_j}, \quad G_k = \rho g_j \beta \frac{\mu_t}{\mathrm{Pr}_t}\frac{\partial T}{\partial x_j}$$

$C_\mu = 0.09$, $Pr_t = 0.9$, $\sigma_\varepsilon = 1.3$, $\sigma_k = 1.0$, $C_{\varepsilon 1} = 1.44$, $C_{\varepsilon 2} = 1.92$, $C_{\varepsilon 3} = 1.0$, $f_1 = 1$, $f_2 = 1$, $E_\varepsilon = 0$, $D_k = 0$

Costa, J.J.; Oliiveira, L.A.; Blay, D. (1999) – *"Test of several versions for the k-ε type turbulence modelling of internal mixed convection flows"* – International Journal of Heat and Mass Transfer, 42(23):4391-4409

Equations manipulation

The *S-shaped* profile can be obtained/simulated by manipulating: the **damping functions** and the **dynamic viscosity** (both the terms $\boldsymbol{\Gamma_\Phi}$ and $\boldsymbol{S_\Phi}$)

Low-Reynolds k-ε models

General transport equation

$$\frac{\partial}{\partial x_i}(\rho u_i \phi) = \frac{\partial}{\partial x_i}\left(\Gamma_\phi \frac{\partial \phi}{\partial x_i}\right) + S_\phi$$

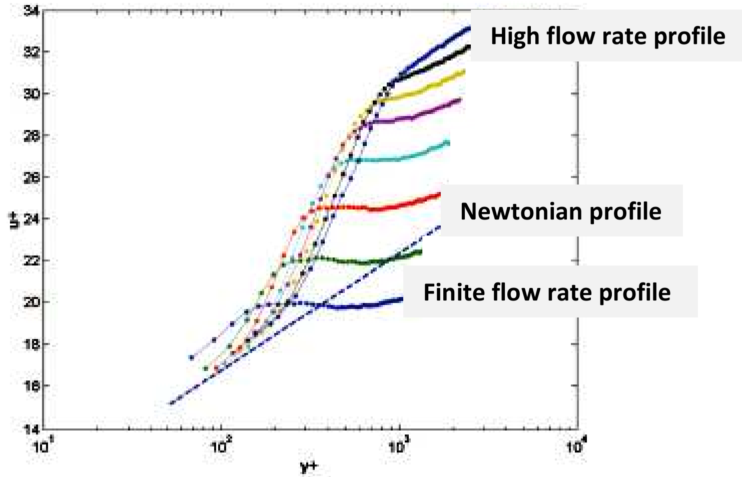

Figure 3 – Dimensionless velocity profiles according to Jäsberg (2007).

Jäsberg, A. (2007) – *"Flow Behavior of Fibre suspensions in Straight Pipes: New Experimental Techniques and Multiphase Modeling"*. PhD Dissertation, Faculty of Mathematics and Science of the University of Jyväskylä, Jyväskylä, Finland

Low-Reynolds turbulence models

ANSYS FLUENT

Low Reynolds number *k-ε* models

Abid (AB)

Lam-Bremhorst (LB)

Launder-Sharma (LS)

Yang-Shih (YS)

Abe-Kondoh-Nagano (AKN)

Chang-Hsieh-Chen (CHC)

Abid, R. (1993) – *"Evaluation of two-equation turbulence models for predicting transitional flows"* – International Journal of Engineering Science, 31(6):831-840

Lam, C.K.G.; Bremhorst, K. (1981) – *"A modified form of the k-ε model for predicting wall turbulence"* – Transactions of the ASME, 103(3):456-460

Launder, B.E.; Sharma, B.I. (1974) – *"Application of the energy-dissipation model of turbulence to the calculation of flow near a spinning disc"* – Letters in Heat and Mass Transfer, 1(2):131-138a

Yang, Z.; Shih, T.H. (1993) – *"New time scale based k-ε model for near-wall turbulence"* – AIAA Journal, 31(7):1191-1198

Abe, K.; Kondoh, T.; Nagano, Y. (1994) – *"A new turublence model for predicting fluid flow and heat transfer in separating and reattaching flows I: Flow field calculations"* – International Journal of Heat and Mass Transfer, 37(1):139-151

Chang, K.C.; Ssieh, W.D.; Chen, C.S: (1995) – *"A modified Low-Reynolds-Number turbulence model applicable to recirculating flow in pipe expansion"* – Journal of Fluids Engineering, 117(3):417-423

Hsieh, W.D.; Chang, K.C. (1996) – "*Calculation of wall heat transfer in pipe-expansion turbulent flows*" – International Journal of Heat and Mass Transfer, 39(18):3813-3822

Complete set of differential equations

- *Low-Reynolds turbulence k-ε model*

General transport equation

$$\frac{\partial}{\partial x_i}(\rho u_i \phi) = \frac{\partial}{\partial x_i}\left(\Gamma_\phi \frac{\partial \phi}{\partial x_i}\right) + S_\phi$$

Cartesian Coordinates
Steady state
2D geometry

Table 5 – Expressions for the dependent variables, diffusibility term Γ_ϕ and source-term S_ϕ (Wang and Mujumdar 2005).

Transported property	ϕ	Γ_ϕ	S_ϕ
Mass	1	0	0
Momentum in *i*-direction	u_i	$\mu_{ef} = \mu + \mu_t = \mu + f_\mu C_\mu \frac{k^2}{\tilde{\varepsilon}}$	$-\frac{1}{\rho}\frac{\partial p_{ef}}{\partial x_i} - g_i \beta (T - T_{ref}) + \frac{\partial}{\partial x_j}\left(\mu_{ef}\frac{\partial u_j}{\partial x_i}\right)$
Turbulent kinetic energy	k	$\mu_{ef} = \mu + \frac{\mu_t}{\sigma_k}$	$P_k + G_k - \tilde{\varepsilon} + D_k$
Dissipation rate of k	ε	$\mu_{ef} = \mu + \frac{\mu_t}{\sigma_\varepsilon}$	$\frac{\varepsilon}{k}\left(f_1 C_{\varepsilon 1} P_k - f_2 C_{\varepsilon 2} \tilde{\varepsilon} + C_{\varepsilon 1} C_{\varepsilon 3} G_k\right) + E_\varepsilon$
$\mu_t = \rho f_\mu C_\mu \frac{k^2}{\varepsilon}$			
$P_k = \rho \mu_t \left(\frac{\partial u_i}{\partial x_j} + \frac{\partial u_j}{\partial x_i}\right)\frac{\partial u_i}{\partial x_j}$, $G_k = \rho g_j \beta \frac{\mu_t}{Pr_t}\frac{\partial T}{\partial x_j}$; $Pr_t = 0.9$, $C_{\varepsilon 3} = 1.0$			

Wang, S.J.; Mujumdar, A.S. (2005) – *"A comparative study of five low Reynolds number k-ε models for impingement heat transfer"* – Applied Thermal Engineering, 25(1):31-44

Model constants and damping functions

Table 6– Model constants and functions.

Model	D_k	E_ε	ε_w – B.C.	C_μ	$C_{\varepsilon 1}$	$C_{\varepsilon 2}$	σ_k	σ_ε
AB	0	0	$\nu\left(\frac{\partial^2 k}{\partial y^2}\right)$	0.09	1.45	1.83	1.0	1.4
LB	0	0	$\left(\frac{\partial \varepsilon}{\partial y}\right)_w = 0$	0.09	1.44	1.92	1.0	1.3
LS	$2\nu\left(\frac{\partial\sqrt{k}}{\partial y}\right)^2$	$2\mu\nu_t\left(\frac{\partial^2 U}{\partial y^2}\right)^2$	0	0.09	1.44	1.92	1.0	1.3
YS(a)	0	$\mu\nu_t\left(\frac{\partial^2 U}{\partial y^2}\right)^2$	$2\nu\left(\frac{\partial\sqrt{k}}{\partial y}\right)^2$	0.09	1.44	1.92	1.0	1.3
AKN	0	0	$\nu\left(\frac{\partial^2 k}{\partial y^2}\right)$	0.09	1.5	1.9	1.4	1.4
CHC	0	0	$\nu\left(\frac{\partial^2 k}{\partial y^2}\right)$	0.09	1.44	1.92	1.0	1.3

(a) $\mu_t = \rho f_\mu k T_t$; $T_t = \frac{k}{\varepsilon} + T_k$; $T_k = c_k\left(\frac{\nu}{\varepsilon}\right)^{1/2}$; $c_k = 1.0$

Model constants and damping functions

Table 7 – Damping functions.

Model	f_μ	f_1	f_2
AB	$\tanh\left(0.008\ Re_y\right)\left(0+4\,Re_T^{-3/4}\right)$	1.0	$\left[1-\frac{2}{9}\exp\left(-Re_T^2\right)\frac{1}{36}\right]^2$
LB	$\left[1-\exp\left(-0.0165\ Re_y\right)\right]^2\left[1+\frac{20.5}{Re_T}\right]$	$1+\left(\frac{0.05}{f_\mu}\right)^3$	$1-\exp\left(-Re_T^2\right)$
LS	$\exp\left(-\frac{3.4}{\left(1+\frac{Re_T}{50}\right)^2}\right)$	1.0	$1-0.3\exp\left(Re_T^2\right)$
YS	$\left[1-\exp\left(-1.5\times10^{-4}\,Re_y-5\times10^{-7}\,R_y^3-1.0\times10^{-10}\,R_y^5\right)\right]^{1/2}$	1.0	1.0
AKN	$\left\{1-\exp\left(-\frac{y^*}{14}\right)\right\}^2\left[1+\frac{5}{R_t^{3/4}}\exp\left\{-\left(\frac{R_t}{200}\right)^2\right\}\right]$	1.0	$\left\{1-\exp\left(-\frac{y^*}{3.1}\right)\right\}^2\left[1-0.3\exp\left\{-\left(\frac{R_t}{6.5}\right)^2\right\}\right]$
CHC	$\left[1-\exp\left(-0.0215\ Re_y\right)\right]^2\left(1+\frac{31.66}{Re_T^{5/4}}\right)$	1.0	$\left[1-0.01\exp\left(-Re_T^2\right)\right]\left[1-\exp\left(-0.0631\ Re_y\right)\right]$
$Re_T=\frac{\rho k^2}{\mu\varepsilon},\ Re_y=\frac{\rho\sqrt{k}\,y}{\mu},\ Re_\varepsilon=\frac{\rho\left(\frac{\mu\varepsilon}{\rho}\right)^{1/4}y}{\mu}$			

Preliminary studies

- Preliminary results led us to conclude that the models **AB**, **AKN** and **CHC** showed a better fit to the experimental data.

- Models **LS** and **YS** did not converge for the higher concentration.

- Model **LB** showed larger deviations.

Convergence criterion = 1×10^{-5}
Water annulus and non-Newtonian

Mesh independence study

Table 8 – Numerical pressure drop different low-Reynolds turbulence *k-ε* model – Mesh 1.

Case	c (% w/w)	U_{in} ($m \cdot s^{-1}$)	Turbulence Model	y^+ first node	$\Delta P/L_{exp.}$ ($Pa \cdot m^{-1}$)	$\Delta P/L_{num.}$ ($Pa \cdot m^{-1}$)	δ (%)
A1	1.50	4.49	AB	**2.1**	829.05	1801.9	117.4
A2			AKN	**2.0**		1756.2	111.8
A3			CHC	0.9		365.2	56.0
A4		6.21	AB	**3.0**	1288.70	3686.7	186.1
A5			AKN	**2.9**		3531.7	174.1
A6			CHC	**2.8**		3219.4	149.8
A7	2.50	4.90	AB	**2.3**	1578.94	2202.9	39.5
A8			AKN	**2.3**		2195.5	39.1
A9			CHC	**2.2**		2134.5	35.2
A10		5.55	AB	**2.4**	1753.79	2394.1	36.5
A11			AKN	**2.4**		2386.4	36.1
A12			CHC	**2.3**		2330.6	32.9

Mesh 1

Non-uniform mesh 20×54 (*x* and *r*)
interval length ratio R1.10

5. Numerical results

Mesh independence study

Convergence criterion = 1 $\times 10^{-5}$
Water annulus and non-Newtonian

Table 9 – Numerical pressure drop different low-Reynolds turbulence *k-ε* model – Mesh 2.

Case	c (% w/w)	U_{in} ($m \cdot s^{-1}$)	Turbulence Model	y^{+} first node	$\Delta P/L_{exp.}$ ($Pa \cdot m^{-1}$)	$\Delta P/L_{num.}$ ($Pa \cdot m^{-1}$)	δ (%)
B1	1.50	4.49	AB	**0.7**	829.05	1827.8	120.5
B2			AKN	**0.7**		1756.9	111.9
B3			CHC	**0.3**		361.1	56.4
B4		6.21	AB	**1.0**	1288.70	**3608.2**	180.0
B5			AKN	**1.0**		**3476.2**	169.7
B6			CHC	**1.0**		3285.1	154.9
B7	2.50	4.90	AB	**0.8**	1578.94	**2192.5**	38.9
B8			AKN	**0.8**		**2193.4**	38.9
B9			CHC	**0.8**		**2108.3**	33.5
B10		5.55	AB	**0.8**	1753.79	**2386.7**	36.1
B11			AKN	**0.8**		**2383.6**	35.9
B12			CHC	**0.8**		**2310.6**	31.8

Mesh 2

Non-uniform mesh 20×65 (*x* and *r*)

interval length ratio R1.10

Mesh independence study

Convergence criterion = 1 $\times 10^{-5}$
Water annulus and non-Newtonian

Table 10 – Numerical pressure drop different low-Reynolds turbulence *k-ε* model – Mesh 3.

Case	c (% w/w)	U_{in} ($m \cdot s^{-1}$)	Turbulence Model	$y^+_{first\ node}$	$\Delta P/L_{water}$ ($Pa \cdot m^{-1}$)	$\Delta P/L_{exp.}$ ($Pa \cdot m^{-1}$)	$\Delta P/L_{num.}$ ($Pa \cdot m^{-1}$)	δ (%)
C1	1.50	4.49	AB	**0.5**	1885.16	829.05	**1810.5**	118.4
C2			AKN	**0.5**			**1737.8**	109.6
C3			CHC	**0.3**			**359.1**	56.7
C4		6.21	AB	**0.8**	3419.65	1288.70	**3119.5**	142.1
C5			AKN	**0.8**			**3130.0**	142.9
C6			CHC	**0.7**			**3272.1**	153.9
C7	2.50	4.90	AB	**0.6**	2212.55	1578.94	**2084.6**	32.0
C8			AKN	**0.6**			**2117.0**	34.1
C9			CHC	**0.6**			**2014.2**	27.6
C10		5.55	AB	**0.6**	2781.05	1753.79	2405.8	37.2
C11			AKN	**0.6**			2415.2	37.7
C12			CHC	**0.6**			2337.3	33.3

Mesh 3

Non-uniform mesh
20×118 *(x* and *r)*

interval length ratio
R1.05

Mesh independence study

- The **y^+ value** recommended for the low-Reynolds *k-ε* turbulence model is **≈ 1** - **mesh 1 is not appropriate**.

- **Mesh 2 has the nodes more "concentrated" near the wall** which can lead to a less accurate solution near the pipe center.

- **The mesh selected was mesh 3**.

u^+ profiles

● Low Reynolds Number k-e

— Standard high Reynolds k-e - Log Law

Table 11 – Dimensionless velocity profile as a function of dimensionless distance to the pipe wall, **c=1.50%** (w/w) – Mesh 3.

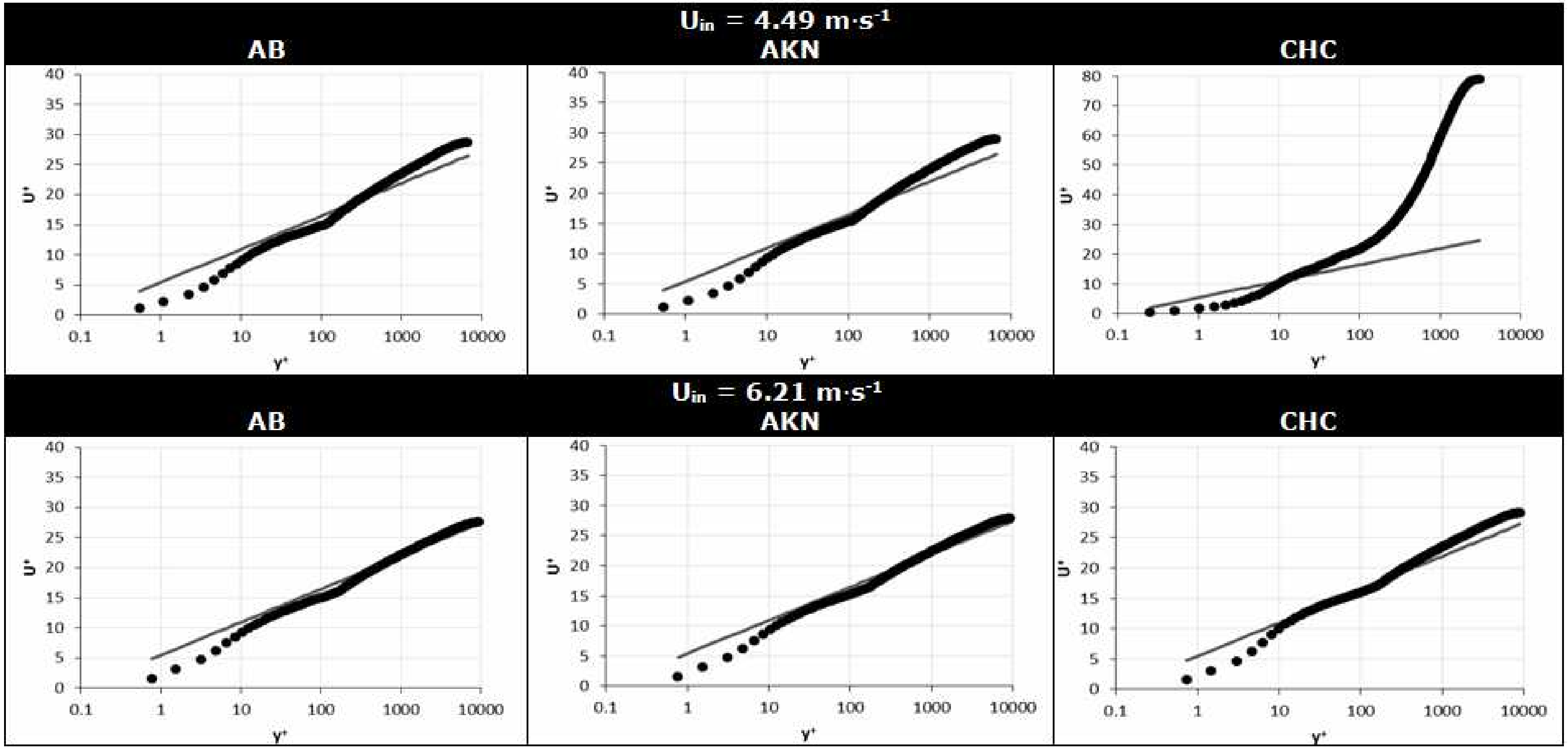

u^+ profiles

● Low Reynolds Number k-e

—— Standard high Reynolds k-e - Log Law

Table 12 – Dimensionless velocity profile as a function of dimensionless distance to the pipe wall, **c=2.50%** (w/w) – Mesh 3.

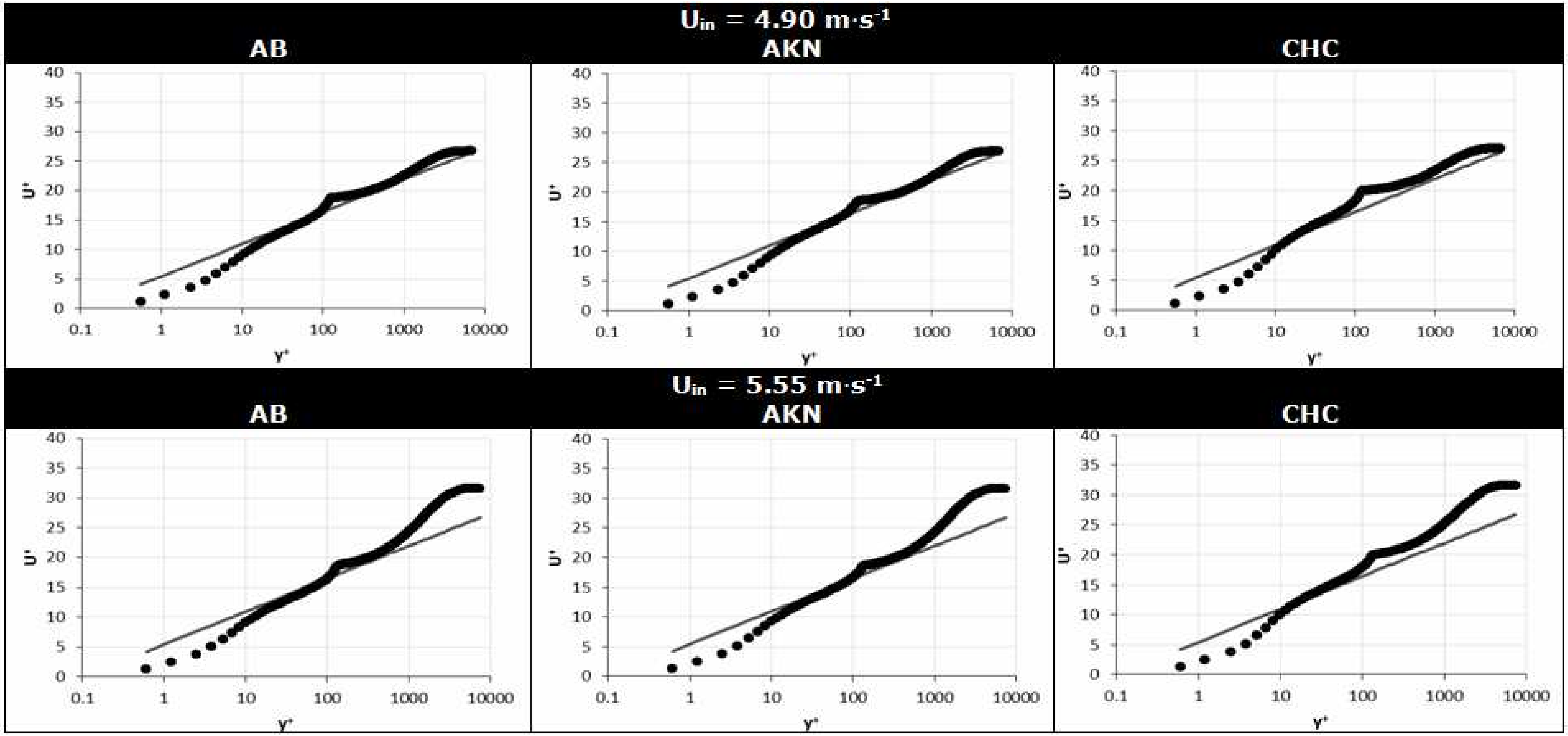

ε profiles

Table 13 – Dissipation rate of turbulent kinetic energy profiles – Mesh 3.

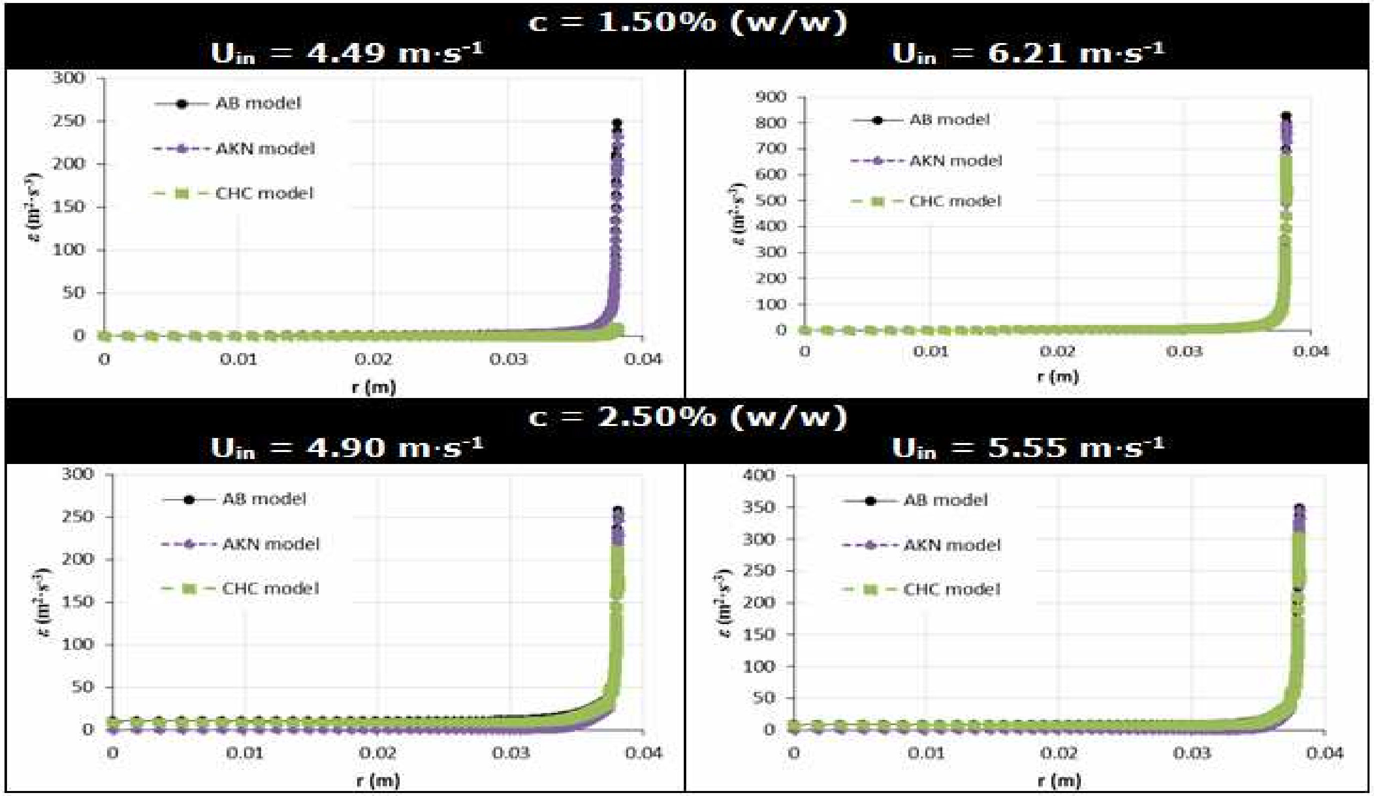

k profiles

Table 14 – Turbulent kinetic energy profiles – Mesh 3.

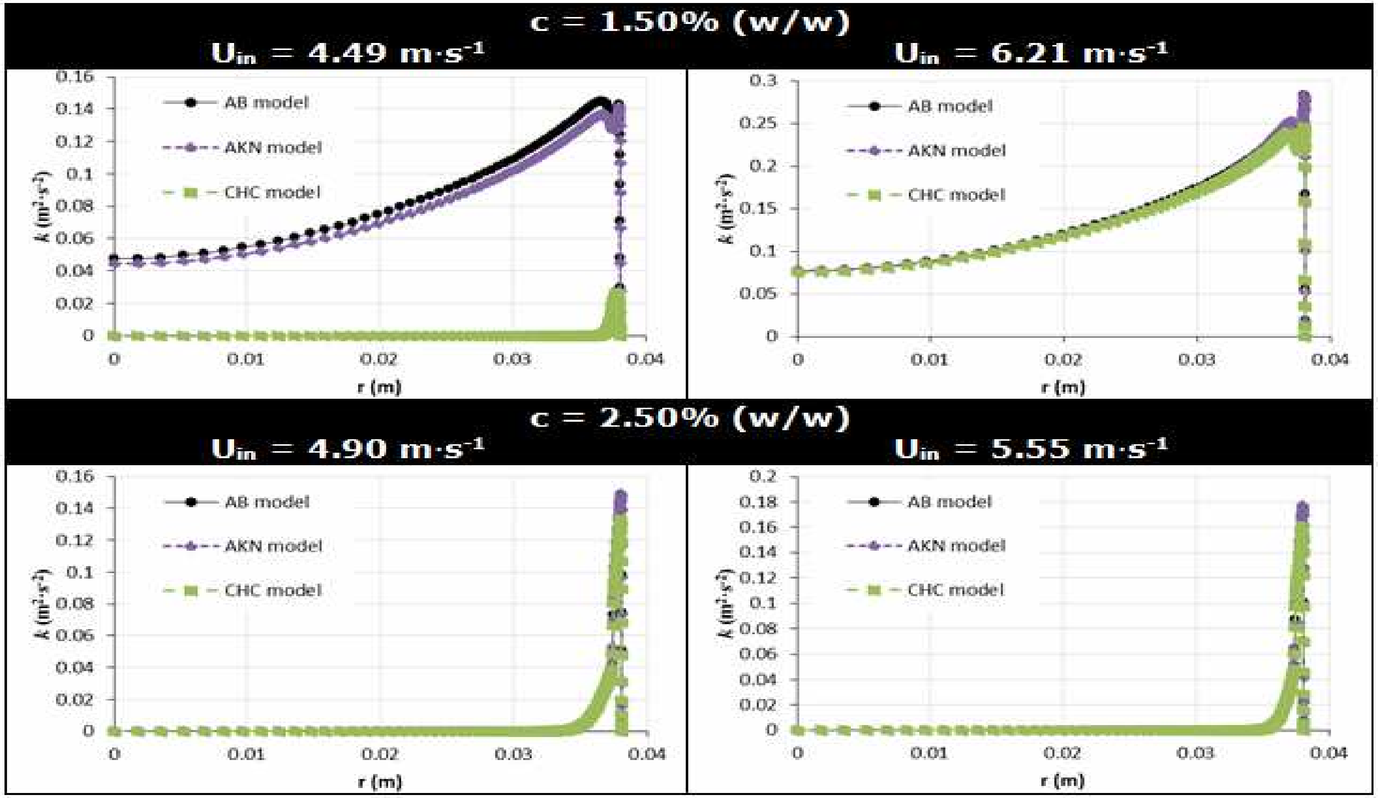

μ profiles

Table 15 – Dynamic viscosity profiles – Mesh 3.

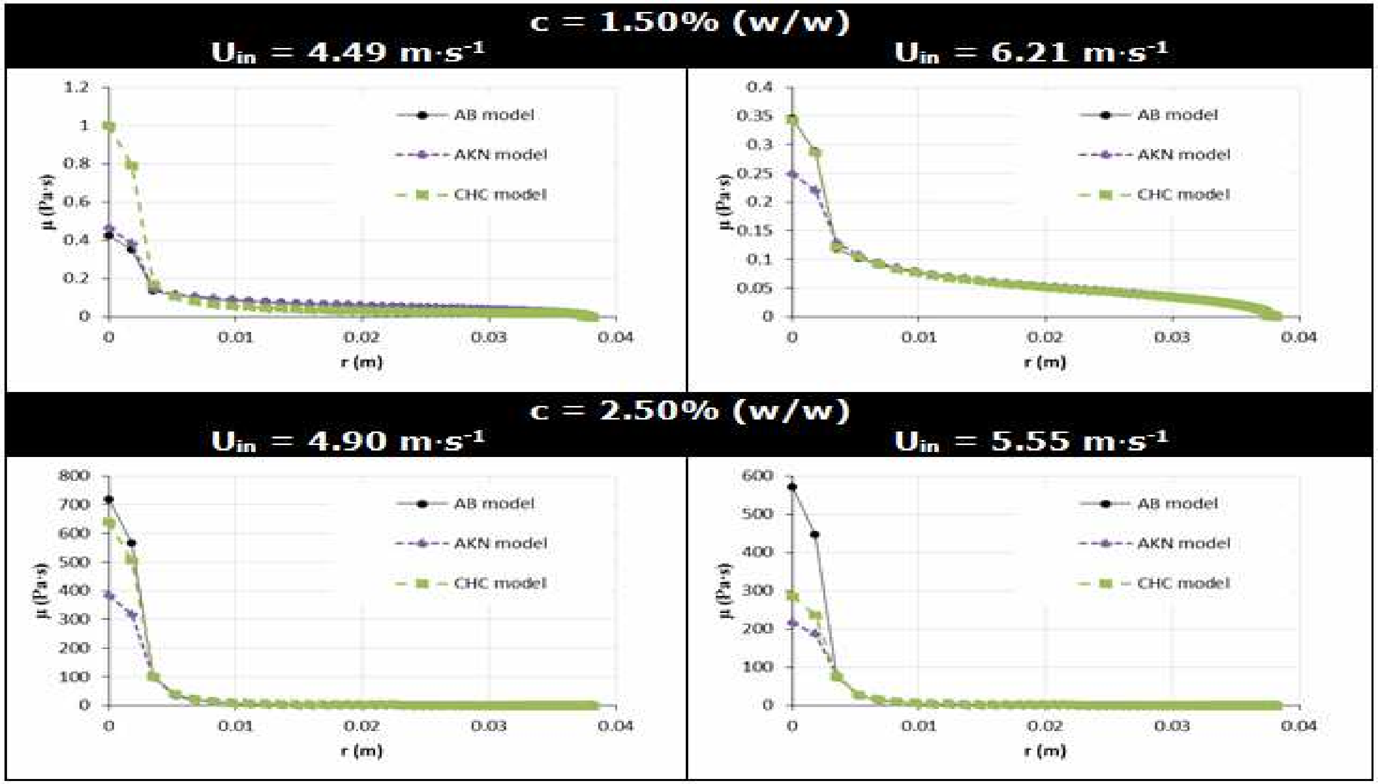

- A ***drag reduction*** can be observed in all cases.

- The **modification on the diffusibility term and source term** (non-Newtonian fluid and low-Reynolds-number k-ε turbulence model) reproduces the *drag reduction* effect.

- The numerical results are **more dependent** on the low-Reynolds-number turbulence model when the **pulp consistency is lower**.

- The **near wall effects are important for pulp flow**. The different models give S-shaped dimensionless velocity profiles mainly, the CHC model.

- **CHC model** appears to **perform better** for the **higher consistencies**. Additionaly, it shows an **increase on turbulence damping**.

- These three models **can be modified** taking into account the modifications presented in **literature for fibers, polymers and particles under turbulent flow with *drag reduction***.

7. Future work

UNIVERSIDADE DE COIMBRA

- Implement the models AB, AKN and CHC using user-defined functions (UDF) in ANSYS Fluent.

- Modify the damping functions (influencing both the diffusibility and source terms) according to information in the literature; namely testing the possibility of using modified damping functions developed for polymer solutions flows or particle suspensions flow (uniform concentration distribution of the particles):

Malin, M.R. (1997) – *"Turbulent pipe flow of power-law fluids"* – International Communications in Heat and Mass Transfer, 24(7):977-988

$$f_\mu = \left[1 - exp\left(-\frac{0.0165\,Re_n}{n^{1/4}}\right)\right]^2\left(1+\frac{20.5}{Re_t}\right)$$

Bartosik, A. – *"Mathematical modelling of slurry flow with medium solid prticles"* – Mathematical Models and Methods in Modern Science, International Conference Mathematical Models and Methods in Modern Science, Spain, 10-12 December, 2011. ISBN 978-1-6-61804-055-8, pp.124-129.

$$f_\mu = 0.09\exp\left[\frac{-3.4\left[1+A_s^3 d^2\left(8-88A_s d\right)C_V^{0.5}\right]}{\left(1+\frac{\mathrm{Re}_t}{50}\right)^2}\right]$$

- Study the influence of constant values on the damping functions f_μ, f_1 and f_2.

Thank you for your attention…

Modelling concentrated fiber suspension flow using different low Reynolds k-ε turbulence models

COST ACTION FP1005
(6th ERCOFTAC SIG43 Workshop)

23-25 October 2013, Udine, Italy

cost